



HAL
open science

Modeling bee movement shows how a perceptual masking effect can influence flower discovery, foraging efficiency and pollination

Ana Morán, Mathieu Lihoreau, Alfonso Pérez Escudero, Jacques Gautrais

► To cite this version:

Ana Morán, Mathieu Lihoreau, Alfonso Pérez Escudero, Jacques Gautrais. Modeling bee movement shows how a perceptual masking effect can influence flower discovery, foraging efficiency and pollination. 2022. hal-03856405

HAL Id: hal-03856405

<https://hal.science/hal-03856405v1>

Preprint submitted on 17 Nov 2022

HAL is a multi-disciplinary open access archive for the deposit and dissemination of scientific research documents, whether they are published or not. The documents may come from teaching and research institutions in France or abroad, or from public or private research centers.

L'archive ouverte pluridisciplinaire **HAL**, est destinée au dépôt et à la diffusion de documents scientifiques de niveau recherche, publiés ou non, émanant des établissements d'enseignement et de recherche français ou étrangers, des laboratoires publics ou privés.

1 **Modeling bee movement shows how a perceptual masking effect can** 2 **influence flower discovery, foraging efficiency and pollination**

3 Ana Morán, Mathieu Lihoreau, Alfonso Pérez Escudero, Jacques Gautrais*

4 Centre de Recherches sur la Cognition Animale (CRCA), Centre de Biologie Intégrative (CBI), Université de
5 Toulouse, CNRS, UPS, 118 route de Narbonne, Bat 4R4, 31062 Toulouse Cedex 9, France

6 * Corresponding author: jacques.gautrais@univ-tlse3.fr

7 **Abstract**

8 Understanding how pollinators move across space is key to understanding plant mating patterns. Bees are
9 typically assumed to search for flowers randomly or using simple movement rules, so that the probability
10 of discovering a flower should primarily depend on its distance to the nest. However, experimental work
11 shows this is not always the case. Here, we explored the influence of flower size and density on their
12 probability of being discovered by bees by developing a movement model of central place foraging bees,
13 based on experimental data collected on bumblebees. Our model produces realistic bee trajectories by
14 taking into account the autocorrelation of the bee's angular speed, the attraction to the nest, and a
15 gaussian noise. Simulations revealed a « masking effect » that reduces the detection of flowers close to
16 another, which may have critical consequences for pollination and foraging success. At the plant level,
17 flowers distant to the nest were more often visited in low density environments, suggesting lower
18 probabilities of pollination at high densities. At the bee colony level, foragers found more flowers when
19 they were small and at medium densities, suggesting that there is an optimal flower size and density at
20 which collective foraging efficiency is optimized. Our results indicate that the processes of search and
21 discovery of resources are potentially more complex than usually assumed, and question the importance
22 of resource distribution and abundance on plant-pollinator interactions.

23 **Keywords:** central place foraging; bee; model simulations; persistent turning walker

24 **Author's summary**

25 Understanding how pollinators move in space is key to understanding plant reproduction, which in turn
26 shapes entire ecosystems. Most current models assume simple movement rules that predict that flowers
27 are more likely to be visited—and hence pollinated—the closer they are to the pollinators' nest. Here we
28 developed an explicit movement model that incorporates realistic features of bumblebees, including their
29 flight characteristics and their tendency to return regularly to the nest, and calibrated it with experimental
30 data collected in naturalistic conditions. This model revealed that the probability to visit a flower does not
31 only depend on its position, but also on the position of other flowers that may mask it from the forager.
32 This masking effect means that pollination efficiency depends on the density and spatial arrangement of
33 flowers around the pollinator's nest, often in counter-intuitive ways. Taking these effects into account will
34 be key for improving precision pollination and pollinator conservation.

35 **Introduction**

36 Pollinators, such as bees, flies, butterflies, but also bats and birds, mediate a key ecosystemic
37 service on which most terrestrial plants and animals, including us humans, rely on. When foraging for
38 nectar, animals transfer pollen between flowers, which facilitates plant reproduction. Understanding how
39 pollinators move, find and choose flowers is thus a key challenge of pollination ecology (1). In particular,
40 this may help predict and act on complex pollination processes in a context of a looming global pollination
41 crisis, when food demand increases and pollinators decline (2,3).

42 Pollinators have long been assumed to move randomly (4–7) or use hard wired movement rules
43 such as visiting the nearest unvisited flower (8), exploiting flower patches in straight line movements (9),
44 navigating inflorescences from bottom to top flowers (10), or using win-stay lose-leave strategies (11).
45 Therefore, pollination models relying on these observations typically predict diffusive movements in every
46 direction (12). However, recent behavioral research shows this is not true when animals forage across large
47 spatial scales (13). In particular, studies using radars to monitor the long distance flight paths of bees

48 foraging in the field demonstrate foragers learn features of their environment to navigate across
49 landscapes and to return to known feeding locations (14,15). This enables them to develop shortcuts
50 between food sources (16) and build efficient multi-location routes (also called “traplines”) minimizing
51 overall travel distances (17,18). These routes are re-adjusted each time a food source is depleted and new
52 ones are discovered (19).

53 How bees learn such foraging routes has been modelled using algorithms implementing spatial
54 learning and memory (20–22). While this has greatly advanced our understanding of bee exploitative
55 movements patterns, none of these models have looked at search behaviors, either assuming insects
56 already know the locations of all available feeding sources in their environment or discover them according
57 to fixed probabilistic laws (i.e. the probability to discover a flower at a given location is proportional to $1/L^2$
58 where L represents the distance to that flower (20–22)). However, experimental data indicate that this is
59 not the case. Firstly, bees, like many pollinators, are central place foragers (i.e., every foraging trip starts
60 and ends at the nest site (23)). This means that their range of action is limited. Recordings of bee search
61 flights, although scarce, show how individuals tend to make loops centered at the nest when exploring a
62 new environment and look for flowers (14,24). These looping movements are not compatible with the
63 assumption that bees make diffusive random walks or Lévy flights (25,26). Secondly, the spatial structure
64 of the foraging environment itself may also greatly influence flower discovery by bees. In particular, the
65 probability of finding a flower heavily depends on the location of the flower visited just before, ultimately
66 influencing the direction and geometry of the routes developed by individuals (17–20,27,28). Since bees
67 are more attracted by larger flowers than by smaller ones (29), this suggests that small isolated flowers
68 could be missed if they are located next to a larger patch. Ultimately, this potential « masking effect » on
69 the probability to visit specific flowers depending on the presence of other flowers around could have
70 important consequences for bee foraging success, for instance by precluding the discovery of some highly
71 rewarding flowers that are isolated or further away from the nest. This could also dramatically influence
72 plant pollination, if bees are spatially constrained to single flower patches and plant outcrossing is limited.

73 Here we developed a model of bee search movement simulating the tendency of bees to make
74 loops around their nest and examined the influence of these looping flights on the probability for bees to

75 discover flowers in environments defined by resources of various sizes and abundances. We hypothesized
76 that considering looping movements characteristic of bee exploratory flights would result in strikingly
77 different predictions than the typical diffusive random walk movements. We also described perceptual
78 masking effects by which the probability of finding given flowers is affected by the presence of others, and
79 analyzed their consequences on discovery rates, bee foraging efficiency and plant pollination success.

80 **The model**

81 **Description**

82 Our model is an extension of the Persistent Turning Walker (PTW) developed by Gautrais et al. (30) to
83 model fish movements in a tank. For the sake of simplicity, here we modelled bee movements in 2D,
84 neglecting altitude. We assumed that bees fly at constant speed and with varying angular speed, $\omega(t)$,
85 which is governed by

$$86 \quad d\omega(t) = -\gamma[\omega(t) - \omega^*(t)]dt + \sigma dW(t), \quad (1)$$

88 where γ is an auto-correlation coefficient and $\sigma dW(t)$ introduces a gaussian noise, governed by a
89 Wiener process (31). The two terms of Equation 1 have opposing effects: The first term pushes the angular
90 speed towards a target angular speed, $\omega^*(t)$, with a strength controlled by the auto-correlation coefficient
91 γ . The second term introduces noise in the angular speed making bees change direction. Therefore, high
92 values of γ lead to smoother and more predictable trajectories. Setting $\omega^*(t) = 0$ leads to a trajectory with
93 no preferred direction, whose angular speed changes smoothly around zero. This is the simplest condition,
94 resembling a diffusive process in which the animal moves aimlessly and gets further and further from its
95 initial position as time goes by (32–37).

96 We modelled central place foraging by adding an attraction component to the model in order to
97 make bees return to the nest after a certain amount of time. To implement the return to the nest we
98 assumed that bees can locate the direction of their nest at any time using path integration (i.e. navigational
99 mechanism by which insects continuously keep track of their current position relative to their nest position
100 (38)), and define a homing vector, $\vec{H}(t)$ that points towards the nest (13). Then, we assumed that the bee

101 tries to target the angular speed that will align its trajectory with the homing vector, so we modeled the
102 target angular speed as

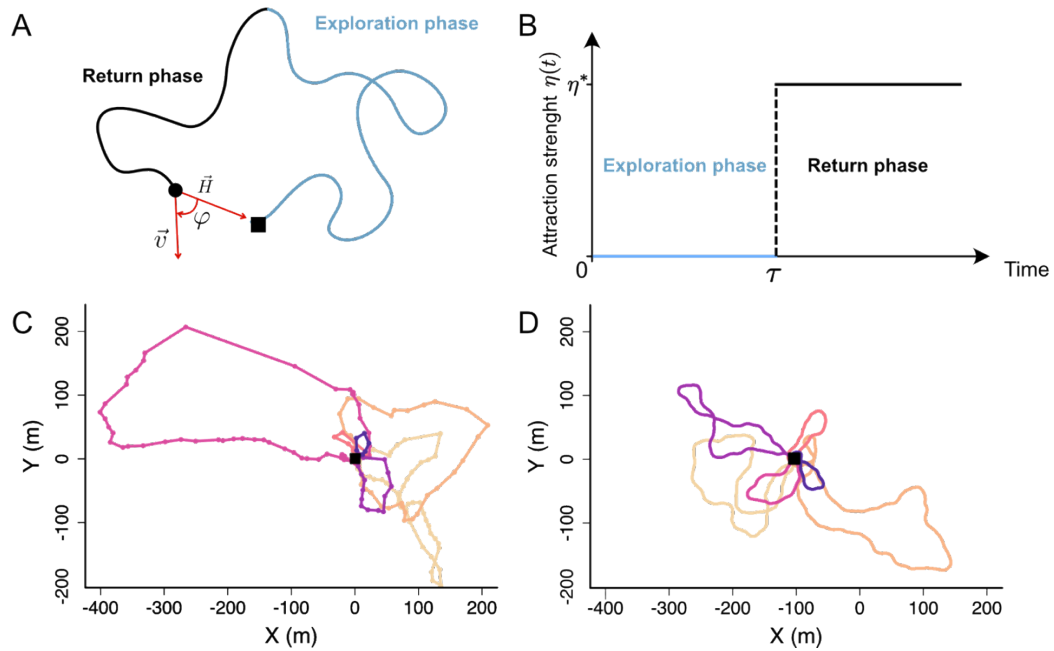
$$\omega^*(t) = \eta(t)\varphi(t), \quad (2)$$

105 where $\varphi(t)$ is the angle between the bee's heading $\vec{v}(t)$ and the homing vector $\vec{H}(t)$ (Fig. 1A), and $\eta(t)$ is
106 the attraction strength that controls a switch between the exploration and return phases: During the initial
107 exploration phase we make $\eta(t) = 0$, so that bees explore randomly and distance themselves from the nest,
108 while during the return phase we make $\eta(t) = \eta^* > 0$, so that the bee has a tendency to turn towards the
109 nest. We assumed that bees switch instantaneously between the exploration and return phases, so

$$\begin{cases} \eta(t) = 0 & \text{if } t < \tau \\ \eta(t) = \eta^* & \text{if } t \geq \tau \end{cases} \quad (3)$$

111 where τ is the time at which the switch happens (Fig. 1B). This switch may happen at any time, with a
112 constant probability per unit time, p_{return} . This means that the switching times are exponentially distributed,
113 with an average time of approximately $1/p_{\text{return}}$.

115 The model therefore has four main parameters: The auto-correlation (γ) and the randomness (σ)
116 control the characteristics of the flight, while the probability to return (p_{return}) and the strength of the
117 attraction component (η^*) control the duration of each exploration trip. Here we have described the
118 continuous version of the model, but to implement it numerically we discretized it in finite time steps (see
119 Methods).



120

121 **Fig 1. Illustration of the model. (A)** Example of theoretical trajectory. Blue line: Trajectory during the

122 exploration phase. Black line: Trajectory during the return phase. Black circle: bee. Black square: nest. H is

123 the homing vector pointing towards the nest. \vec{v} is the heading of the bee. φ is the angle between \vec{v} and \vec{H} .

124 **(B)** Evolution of the return strength (η) over time. At time = τ , η switches from 0 (no attraction) to η^* . **(C)**

125 Example of an experimental trajectory (39). Each dot represents the position of a bee recorded by a

126 harmonic radar approximately every 3s. Different colors represent different loops around the nest. The

127 sequential order of the loops is represented by the color gradient where the first loops have lightest colors

128 (yellow to purple). **(D)** Same as C, but for a simulated trajectory with parameters $\gamma = 1.0 \text{ s}^{-1}$, $\sigma = 0.37 \text{ rad/}$

129 $\text{s}^{1/2}$, $\rho_{\text{return}} = 1/30 \text{ s}^{-1}$ and $\eta^* = 0.2 \text{ s}^{-1}$.

130 Calibration with experimental data

131 In principle, our model can describe search movements of any central place forager. Here we explored its

132 properties focusing on a model species for which we had access to high-quality experimental data: the

133 buff-tailed bumblebee *Bombus terrestris*. We used the dataset of Pasquaretta et al. (39) in which the

134 authors used a harmonic radar to track 2D exploratory flight trajectories of bees in the field. Bees carrying

135 a transponder were released from a colony nest box located in the middle of a large and flat open field,

136 and performed exploration flights without any spatial limitation. The radar recorded the location of the

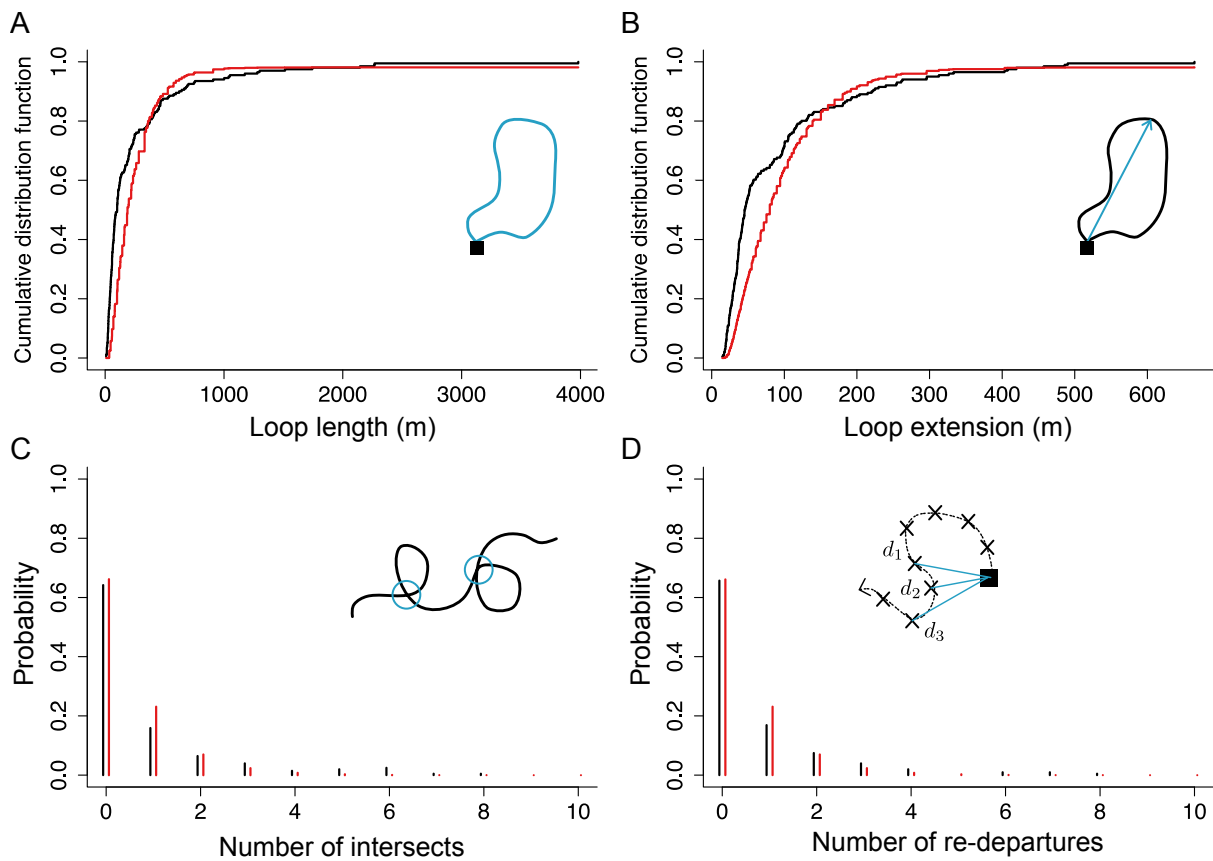
137 bees every 3.3s over a distance of ca. 800 m (Fig 1C). In these experiments the bees were tested until they
138 found artificial flowers randomly scattered in the field. We used 32 radar tracks for 18 bees.

139 To quantify the experimental trajectories, we first divided tracks into "loops", each loop being a
140 segment of trajectory that starts and ends in the nest (Fig 1C). This extraction yielded 207 loops. We then
141 computed four observables for each loop (Fig 2):

- 142 • Loop length: Total length of the trajectory for a given loop (Fig. 2A).
- 143 • Loop extension: Maximum distance between the bee and the nest for a given loop (Fig.
144 2B).
- 145 • Number of intersections: Number of times the loop intersects with itself (Fig. 2C).
- 146 • Number of re-departures, where a re-departure is defined as three consecutive positions
147 such that the second position is closer to the nest than the first one, but the third is again
148 further away than the second. These events indicate instances in which the bee seemed
149 to be returning towards the nest and turned back (Fig. 4D).

150 We extracted these four parameters from each loop and found substantial variability in all of them (Fig. 3,
151 black lines). We then used this information to find the optimal model parameters, aiming to describe not
152 only the average value of each observable, but also their variability. To do so, we performed simulations
153 covering exhaustively all relevant combinations of our four parameters. For each combination of
154 parameters, we simulated 1000 loops, extracted the distributions for the four observables, and chose the
155 parameter combination that best approximated the experimental distributions for the four observables
156 (see Methods). This procedure resulted in the optimal parameters $\gamma = 1.0 \text{ s}^{-1}$, $\sigma = 0.37 \text{ rad/s} * \text{ s}^{1/2}$, $p_{\text{return}} =$
157 $1/30 \text{ s}^{-1}$ and $\eta^* = 0.2 \text{ s}^{-1}$, which give a good approximation to the experimental distributions of observables

158 (Fig. 2, red lines), and trajectories that qualitatively resemble the experimental ones (Fig. 1D)



159

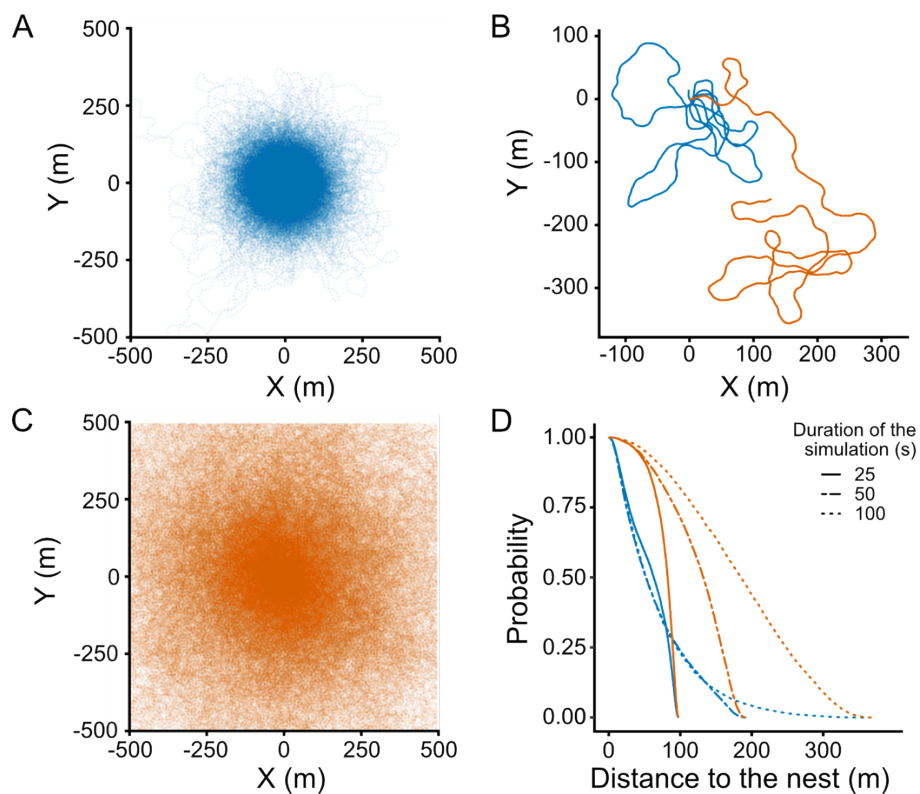
160 **Fig 3. Distributions of the four observables, for experimental and simulated data.** Black lines:
 161 experimental data. Red lines: model predictions using the optimal $\gamma = 1.0 \text{ s}^{-1}$, $\sigma = 0.37 \text{ rad/s} * \text{ s}^{1/2}$, $\rho_{\text{return}} =$
 162 $1/30 \text{ s}^{-1}$ and $\eta^* = 0.2 \text{ s}^{-1}$. Insets: Schematic of each observable. **(A)** Cumulative distribution function of loop
 163 lengths for our full dataset. **(B)** Same as A, but for the loops extension. **(C)** Probability distribution of the
 164 number of trajectories intersects per 100m traveled. **(D)** Same as C, but for the number of re-departures
 165 per 100 m traveled.

166 Model predictions

167 Attraction to the nest limits the exploration range of bees

168 An unrealistic feature of existing diffusive models is their long-term behavior: If given enough time, the
 169 forager reaches extremely far distances with respect to the nest, never returning to it. To measure the
 170 impact of central place foraging on bee exploration range, we compared our model with attraction to the
 171 nest to an alternative one in which the attraction is absent (i.e., making $\eta^* = 0$ in Equation 3). We then

172 simulated 1000 trajectories with each model for different amounts of time, and studied how the
173 distribution of bees around the nest changes over time.
174 This analysis revealed two main effects of the attraction component. First, it retains bees tightly localized
175 around the nest (~250m) (Fig. 3A-B, blue). Second, it makes the distribution of bees stationary: In a
176 model without attraction, bees constantly wander away from the nest, and their distribution depends on
177 how much time we allow for the bee to explore, becoming wider as time goes by (Fig. 3B-C, orange). In
178 contrast, the attraction component makes the forager return to the nest periodically, so the distribution
179 remains constant once the forager has had enough time to perform more than one loop on average (Fig.
180 3D, blue)



181
182 **Fig 3. Probability of presence of a bee around the nest. (A)** Overlay of 1000 trajectories with attraction to
183 the nest ($\eta^* = 0.2 \text{ s}^{-1}$) simulated during 900 s. **(B)** Same as A but without attraction to the nest ($\eta^* = 0$) **(C)**
184 Probability to find a bee below a given distance to the nest (i.e., inverse cumulative probability distribution
185 for the distance to the nest) after different amounts of time. **(D)** Example trajectories with and without
186 attraction, simulated during 500 s. The nest is located at (0,0). Blue: model with attraction. Orange: model
187 without attraction.

188 **Distant flowers are more often visited in low-density environments**

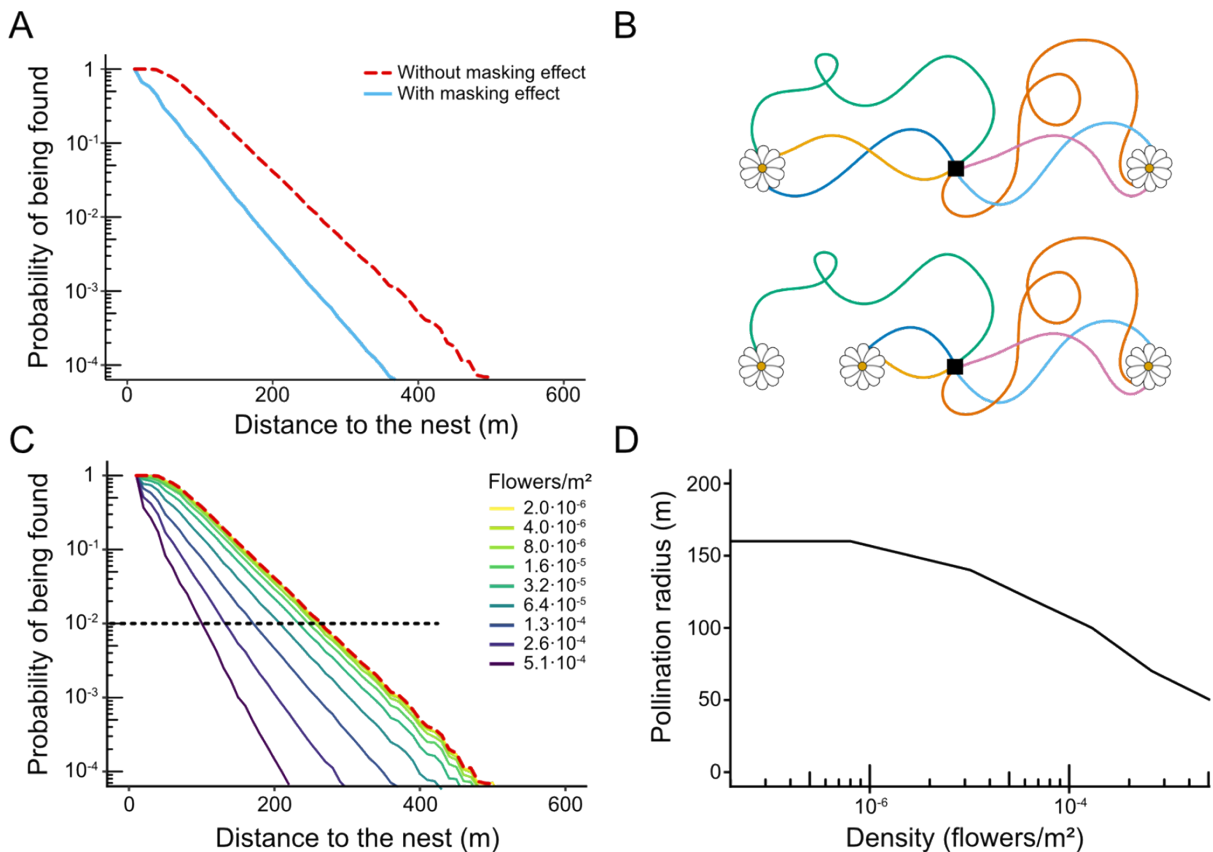
189 A key consequence of bee movement is its influence on plant reproduction through pollen dissemination.
190 We estimated the probabilities of flowers to be discovered (and thus pollinated) by bees in a field
191 characterized by a random and uniform distribution of flowers, an average density of $1.3 \cdot 10^{-4}$ flowers/m²
192 and a diameter of 70cm (for the sake of simplicity here a “flower” is equivalent to a feeding location, which
193 may be a single flower or a plant containing several ones). We assumed that a flower was visited whenever
194 its distance to the bee’s trajectory was below a threshold, given by the bee’s visual perception range (see
195 Methods). We focused on vision rather than olfaction because vision is the main sense that bees use to
196 accurately navigate the last meters towards a particular flower, while olfaction is used at a broader spatial
197 scale (23). Using these conditions, we simulated 1000 foraging trips, each of them lasting 900 seconds, and
198 for each flower we computed the probability to be found in a given trip (i.e., the proportion of simulations
199 in which the trajectory overlaps with the flower’s area of attraction). This probability falls exponentially
200 with the distance between the flower and the nest (Fig. 4A, red line).

201 However, this simulation does not take into account the fact that the probability of visiting a flower
202 does not only depend on its distance to the nest, but can also be influenced by the presence of other
203 flowers around. This dependence exists because a bee that finds a flower does not continue its trajectory,
204 but will rather stop to collect nectar. Once nectar collection is over, the bee may continue exploring, but
205 after visiting a few flowers the bee returns to the nest to unload its crop. For example, in a scenario where
206 there are just 2 flowers equidistant to the nest, both flowers should be visited equally. However, if another
207 flower is added, it can capture visits that would otherwise visit one of the original flowers, reducing the
208 probability that it’s discovered (Fig. 4B). We call this “the masking effect” (Figure 4B).

209 In order to model this masking effect in a simple way, we assumed that each bee returns to the
210 nest after discovering a single flower. The first qualitative consequence of the masking effect is to reduce
211 the probability that flowers distant to the nest are discovered (Fig. 4A, blue). The second consequence is
212 that it introduces a dependence of flower density on pollination efficiency. In the absence of masking, only
213 two factors determine the probability that a flower is discovered: its size (which determines the distance
214 from which it can be perceived) and its distance to the nest. In contrast, when masking is taken into

215 account, the number of visits also depends on the overall density of flowers in the environment, falling
 216 more sharply with distance when this density is higher (Fig. 4C).

217 This dependence with flower density means that the area around the nest where flowers have a
 218 high probability of being pollinated depends on flower density. To estimate the size of this area, we set a
 219 threshold at a probability of 10^{-2} per trip (black dotted line in Fig. 4C), and computed the “pollination
 220 radius” as the distance at which flowers’ probability of being discovered remains above this threshold,
 221 assuming than one visit is enough for pollinating a plant. At low flower densities the pollination radius
 222 reaches 160 meters, and is limited by the bees’ exploration range (i.e., their tendency to return to the nest
 223 after a certain time, even if no flowers have been found; compare this radius with the distribution in Fig.
 224 3C). Due to the masking effect, the pollination radius decreases as flower density increases (Fig. 4D).



225

226 **Fig 4. Predicted pollination efficiency. (A) Probability that a flower is found as a function of its distance**
 227 **to the nest.** We simulated exploration trips in a field of uniformly distributed flowers with density $1.3 \cdot 10^{-4}$
 228 flowers/m² and flower size 70 cm. For each flower, we computed the probability that it was found in each
 229 exploration trip, and we show this probability as a function of the distance between the flower and the

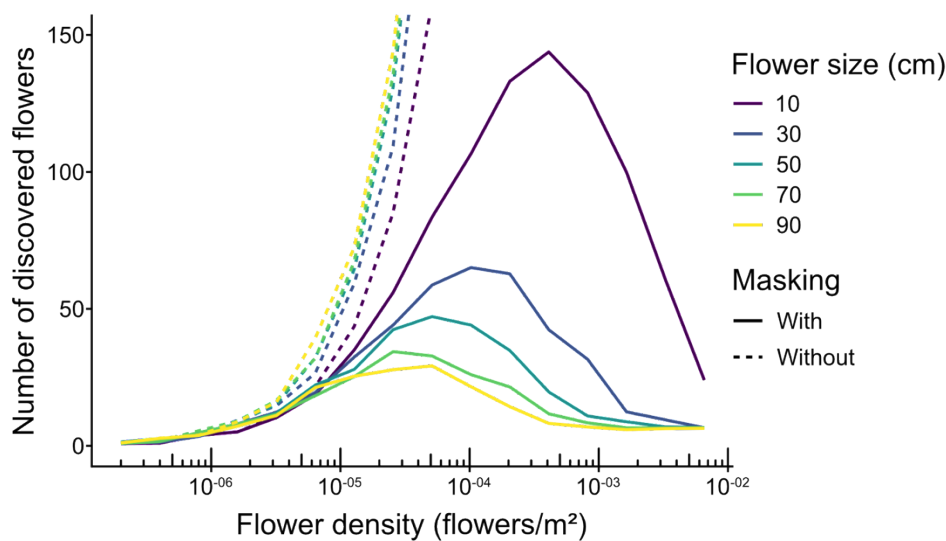
230 nest. Results computed over 6000 simulated trips of 900s in 10000 environments for each density. Red
231 line: Probability calculated without taking into account the masking effect. Blue line: Probability calculated
232 taking into account the masking effect (i.e., only counting the first flower that was discovered in each trip).
233 **(B) Illustration of the masking effect.** The probability of finding a flower depends on the presence of other
234 flowers. In a scenario where there are just 2 flowers equidistant to the nest, both flowers should be visited
235 equally (top). However, if another flower is added, it can capture visits that would otherwise visit one of
236 the original flowers (bottom). Black square: nest. **(C)** Same as (A), but for different flower densities. Red
237 dotted line: Probability calculated without taking into account the masking effect. This probability is
238 independent of the density of flowers. Solid lines: Probability calculated taking the masking effect into
239 account. Black dotted line: threshold probability at which we consider an area that has a high probability
240 of being pollinated. **(D)** Radius of the area around the nest that has a high probability of being pollinated
241 (i.e., where the probability that flowers are discovered is above 10^{-2}) as a function of flower density.

242 **Bees find more flowers at intermediate densities**

243 We then explored potential influences of the masking effect on the foraging success of the bees. This
244 success depends on the number of flowers discovered collectively by all the bees of a colony, because a
245 flower discovered and exploited by a bee will be at least partially depleted, giving little additional benefit
246 to later visitors. For this reason, what counts is not the total number of visits that bees perform, but rather
247 the total number of different flowers discovered by the colony. One would expect that higher flower
248 density would make it easier for the colony to discover a higher number of flowers, but our model showed
249 a counterintuitive effect: Because of the masking effect, higher flower density may result in fewer
250 discovered flowers.

251 To study this effect, we computed the total number of flowers discovered by a bee colony as a
252 function of density and flower size. We considered a field with flowers of a given size uniformly and
253 randomly distributed with a given flower density, simulated 1000 exploration trips, and counted the
254 number of flowers that were discovered at least once. When we performed this simulation neglecting the
255 masking effect (i.e., assuming that a bee discovers all the flowers that intersect with its trajectory, not being

256 affected by such discoveries), we found that the number of flowers discovered increased with flower
257 density and flower size, as these factors make flowers more plentiful and easier to find (Fig. 5, dashed
258 lines). However, the masking effect reverses this trend (Fig. 5, solid lines): For low densities, the masking
259 effect is weak and the number of discovered flowers increases with density, but at high flower densities
260 bees become “trapped” around the nest by the flowers immediately surrounding it, which accumulate
261 most of the visits. Therefore, there is an optimum density that results in the highest number of different
262 flowers discovered. Since the masking effect is stronger for larger flowers, the effect of size also reversed,
263 with the number of discovered flowers decreasing as flower size increases (Fig. 5, solid lines).



264
265 **Fig 5. Number of different flowers discovered by a group of bees as a function of flower density.** Number
266 of different flowers discovered in 1000 exploration trips of 900 s, in an environment with randomly
267 distributed flowers. Results are averaged over 10 simulations, keeping the environment fixed for every
268 simulation. Solid lines: Probability calculated taking into account the masking effect (i.e., only counting the
269 first flower that was discovered in each trip). Dotted lines: Probability calculated without taking into
270 account the masking effect.

271 Discussion

272 How pollinators search for flowers is of fundamental importance but remains poorly understood. Here we
273 developed a realistic model of bee search movements based on their observed tendency to make
274 exploratory loops that start and end at their nest location. Our model, calibrated with real behavioral data,

275 produces two-dimensional trajectories with progressive changes of direction driven by the continuous
276 evolution of the angular velocity $\omega(t)$. Using this approach, we documented a neglected yet potentially
277 fundamentally important effect for bee foraging success and pollination: a perceptual masking effect that
278 influences the probability of bees to discover flowers depending not only based on their size and spatial
279 location, but also on the presence and characteristics of other flowers around them.

280 Previous models assume that bees explore the environment randomly using Lévy flights or other
281 diffusive processes (12,21,22). In a diffusive model, individuals are able to wander away from the nest
282 indefinitely if given enough time. In contrast to these models, our model replicates looping trajectories
283 observed in real bees (14,40), which confines the presence of individuals around a nest. As a consequence
284 of the periodic returns of bees to the nest, their distribution becomes independent of the time given to
285 explore. This result has the important consequence that, under the assumptions of our model, longer
286 simulation durations will result in a more thorough exploitation and pollination of the area around the nest,
287 but not in a larger area being exploited and pollinated.

288 By explicitly simulating individual trajectories in complex environments, our model revealed how
289 the presence of a flower may decrease the probability of discovering another. We named this phenomenon
290 a “perceptual masking effect” and explored its consequences in the probability of bees to discover flowers,
291 ultimately extrapolating on pollination and bee foraging success. At the plant level, flowers distant to the
292 nest were more often visited in low density environments, suggesting lower probabilities of pollination at
293 high densities. Therefore, the area that is pollinated around the nest decreases when the flower density
294 increases. The overall distribution of flower patches directly impacts their pollination and should be taken
295 into account when designing strategies for crop production and assisted pollination. At the bee colony
296 level, insects tended to find more flowers when they were small and at medium densities, suggesting that
297 there is an optimal flower size and density at which collective foraging efficiency is optimized (although the
298 effect of size on foraging efficiency will be compounded with the greater reward provided by bigger flowers
299 on average). The perceptual masking effect may also have an impact on site learning and the formation of
300 traplines: At different scales, flower patches may not be discovered in the same order and the probability
301 of forming an optimal route may depend on the scale at which exploration occurs.

302 Our search model is a scaffold for future characterization of the movement of bees across time
303 and landscapes. Although we limited our study to flower discovery probability, and therefore only provided
304 predictions for first flower discovery, the model could be used to investigate the full foraging trips of bees,
305 and how they change through time as bees acquire experience with their environment and develop spatial
306 memories (13). It would be particularly interesting to integrate this exploration model into existing learning
307 exploitation models proposed to replicate route formation by bees (20–22). Once a flower is discovered,
308 its location can be learned, and new exploration may start, ultimately allowing for the establishment of
309 traplines. This would be modelled via a modification of the attraction component, which can be modified
310 to point towards previously-discovered flowers instead of the nest. Importantly, model predictions (flower
311 discovery probability, visitation order, flight trajectories) can be experimentally tested and the model
312 calibrated for specific study species. This will facilitate improvement and validation for potential
313 applications. For instance, robust predictive models of bee movements including both exploration and
314 exploitation would be particularly useful for improving precision pollination (to maximize crop pollination),
315 pollinator conservation (to ensure population growth and maintenance), but also in ecotoxicology (to avoid
316 exposure of bees to agrochemicals) and legislation (to avoid unwanted gene flow between plants). Beyond
317 pollinators, our minimal persistent turning walker model could be calibrated to apply to a wide range of
318 species, providing a scaffold for further exploration of the broader interactions between central place
319 foraging animals and their environment.

320 More broadly speaking, the Persistent Turning Walker model has inspired some developments in
321 other animals, especially fish (41–43) as well as in robotics (44) where it has been proven to display better
322 coverage properties than classical random walks(45). The addition of the attraction component paves the
323 avenue for further developments of this model in these areas as well.

324

325 **Methods**

326 The codes used to perform all the simulations, data analyses and figures are available in the Supplementary
327 Information (Zip file S3).

328 **Modeling nest and flower detection**

329 Bumblebees can detect an object when it forms an angle of 3° on the retina of their compound eyes (46).
330 Therefore, for every model simulation, we set the flowers' size and calculated the distance at which the
331 bees are able to detect them. We call this the "perception distance". We considered that a bee visited a
332 flower when it was located at a distance to the bee inferior to the perception distance. We did not take
333 into account the olfactory perception since it could be less reliable because of other factors like wind
334 direction and the flower's species. However, if taken into account, it would only impact the perception
335 distance of the flowers and the results would not be qualitatively different.

336 **Analysis of experimental data**

337 We used the dataset of Pasquaretta et al. (39) in which the authors tracked exploratory flight trajectories
338 of bumblebees in the field with a harmonic radar. Bees carrying a transponder were released from a colony
339 nest box located in the middle of a large and flat open field, and performed exploration flights without any
340 spatial limitation. The radar recorded the location of the bees every 3.3s over a distance of ca. 800 m, and
341 with an accuracy of approximately 2 m (14). The bees were tested until they found one of three 20-cm
342 artificial flowers randomly scattered in the field. The position of these flowers was changed whenever one
343 of them was found to prevent the bees from learning their location, but their presence may still affect the
344 bees' trajectories. We first attempted to control for this factor by removing all trajectories where bees
345 passed near an artificial flower, but this introduced a significant bias towards short trajectories, because
346 bees are less likely to find a flower when they stay near the nest. Therefore, we used the full dataset, and
347 in order to remove the effect of the bees hovering around and exploiting the artificial flowers, we
348 summarized all the points detected in an area within 6 m of an artificial flower as a single point at the
349 location of the flower. This threshold of 6 m was derived from a 4 m perception distance corresponding to
350 20 cm flowers, plus 2 m to account for the experimental noise. All trajectories are given in S2-section V.

351 **Dividing trajectories into loops**

352 In order to quantify the trajectories, we divided the tracks into "loops". We defined a loop as a fragment
353 of a trajectory that starts when the bee leaves that nest and finishes when it enters back. The colony nest
354 box used in the experiments was rectangular, with a diagonal of 37 cm, meaning that the bees were able
355 to see it at approximately 7m. However, in this case we set a higher threshold of 13 m to avoid including

356 learning flights (i.e., flights during which the bee makes characteristic loops to acquire visual memories of
357 target locations such as the nest for navigation (38) into the set of exploratory data. While our model does
358 not produce learning flights, for consistency we also used the 13-m radius around the nest in our
359 simulations.

360 **Model simulations**

361 All simulations start at the nest (which is located at position 0,0), with a random initial direction, and with
362 zero angular velocity. To simulate the trajectories, we discretized the model using the on a time step $\Delta t =$
363 0.01. Therefore, at every step we calculated the direction $\theta(t + \Delta t)$ as

$$364 \quad \theta(t + \Delta t) = \theta(t) + \omega(t)\Delta t. \quad (M1)$$

366 We then calculated the velocity $v(t + \Delta t)$ with

$$367 \quad \vec{v}(t + \Delta t) = v \begin{pmatrix} \cos(\theta(t + \Delta t)) \\ \sin(\theta(t + \Delta t)) \end{pmatrix}, \quad (M1)$$

369 where v is the speed, which is a constant in our model. Then, the new position is

$$370 \quad \vec{x}(t + \Delta t) = \vec{x}(t) + \vec{v}(t)\Delta t. \quad (M2)$$

372 Lastly, we calculated the angular speed $\omega(t + \Delta t)$. For this, we used the Green functions for
373 Ornstein-Uhlenbeck processes over Δt (see (30) for details), obtaining

$$374 \quad \omega(t + \Delta t) = \omega(t)e^{-\gamma\Delta t} + \omega^*(1 - e^{-\gamma\Delta t}) + \varepsilon, \quad (M3)$$

376 where ω^* is the target angular speed (governed by Equations 2 and 3), and ε is a random number
377 governed by a Gaussian distribution with mean 0 and variance

$$378 \quad s^2 = \sigma^2 \frac{1 + e^{-2\gamma\Delta t}}{2\gamma}. \quad (M4)$$

380 **Parameter fitting**

381 In order to fit the parameters of the model, we explored systematically all relevant combinations within
382 the relevant range for each parameter. To do this more efficiently, we substituted the variance of the noise
383 introduced by the Wiener's process (σ) for the variance of ω , which has a more direct impact on the
384 experimental data. These two variables are related by (30):

$$385 \quad \text{Var}(\omega) = \Omega = \frac{\sigma^2}{2\gamma}.$$

386 We also defined

$$387 \quad \alpha = \frac{1}{\text{P}_{\text{return}}}.$$

388 We simulated 10^3 loops using 6160 different combinations of the parameters of the model ($\gamma, \Omega, \alpha, \eta^*$)

- 389 • $\gamma \in (0.5, 0.6, 0.7, 0.8, 0.9, 1.0, 1.1, 1.2, 1.3, 1.4, 1.5)$
- 390 • $\Omega \in (0.01, 0.03, 0.05, 0.06, 0.07, 0.08, 0.09, 0.1, 0.125, 0.15)$
- 391 • $\alpha \in (10, 20, 25, 30, 35, 40, 50)$
- 392 • $\eta^* \in (0.05, 0.1, 0.15, 0.2, 0.25, 0.3, 0.35, 0.4)$

393 Since the four observables are heterogeneous (two are continuous measures, two are discrete), a
394 cost function averaging over the four had to be designed to ensure that each observable is given the same
395 weight. For each observable, we computed one score as a distance from the simulated set to the observed
396 set. For the two continuous observables (loop length and extension), the score was computed as the area
397 between the observed cumulative distribution function, and the simulated one. For the two discrete
398 observables (numbers of self-intersection and re-departures), the score was computed, as the absolute
399 difference between the two probability distributions. This yielded four distributions of scores over the 6160
400 combinations. Scores were then translated into their quantile their corresponding cumulative distribution
401 (e.g., a score translated into 0.12 means that it is within the lowest 12%). Finally, we retained the
402 combination that yielded the lower quantile averaged over the four observables (see S2, section 2).

403 The best parameters combination was found to be: $\gamma = 1.0 \text{ s}^{-1}$, $\Omega = 0.07 \text{ rad}^2/\text{s}^2$, $\alpha = 30 \text{ s}$ and $\eta^* =$
404 0.2 s^{-1} . It corresponds to the marginal local minima for the four observables (see S2, section 2). Simulated

405 trajectories closely resemble data trajectories (Fig 1B), and the model is able to produce loops with an
406 elongated shape, as well as a diversity of loop lengths.

407 This unique set of parameters assumes that all bees are identical, while in reality inter-individual
408 differences exist (Fig. S1), for example due to differences in age, experience, learning or size (47,48).
409 However, each bee can display a large diversity of loop parameters, covering a similar range as the overall
410 population (Fig SI-1). We therefore considered that separate fits for each individual were not justified. The
411 fact that our model reproduces not only the mean but also the variability of the four observables we
412 defined (Fig. 3) supports this choice.

413

414 **Acknowledgments**

415 We thank Thibault Dubois, Tamara Gómez Moracho, Cristian Pasquaretta, Joe Woodgate, James Makinson,
416 Joanna Brebner and Lars Chittka for sharing their data of bumblebee flight tracks using radar.

417 **Funding**

418 AM was supported by a PhD Fellowship from the French Government. ML was supported by grants of the
419 Agence Nationale de la Recherche (3DNavibee ANR-19-CE37-0024), and the European Commission (FEDER
420 ECONECT MP0021763, ERC Cog BEE-MOVE GA101002644). APE acknowledges funding from a CNRS
421 Momentum grant (<https://www.cnrs.fr/>) and a Fyssen Foundation Research grant
422 (<https://www.fondationfyssen.fr/en/>).

423 The funders had no role in study design, data collection and analysis, decision to publish, or preparation of
424 the manuscript.

425 **References**

- 426 1. Mayer C, Adler L, Armbruster WS, Dafni A, Eardley C, Huang SQ, et al. Pollination ecology in the 21st
427 Century: Key questions for future research. *J Pollinat Ecol.* 2011 Mar 19;8–23.
- 428 2. Buchmann SL, Nabhan GP. The Pollination Crisis. *The Sciences.* 1996;36(4):22–7.
- 429 3. Goulson D, Nicholls E, Botías C, Rotheray EL. Bee declines driven by combined stress from parasites,
430 pesticides, and lack of flowers. *Science.* 2015 Mar 27;347(6229):1255957.

- 431 4. Lenz F, Chechkin AV, Klages R. Constructing a Stochastic Model of Bumblebee Flights from
432 Experimental Data. Aegerter CM, editor. PLoS ONE. 2013 Mar 8;8(3):e59036.
- 433 5. Reynolds AM, Smith AD, Menzel R, Greggers U, Reynolds DR, Riley JR. Displaced honey bees perform
434 optimal scale-free search flights. *Ecology*. 2007 Aug;88(8):1955–61.
- 435 6. Reynolds AM, Smith AD, Reynolds DR, Carreck NL, Osborne JL. Honeybees perform optimal scale-free
436 searching flights when attempting to locate a food source. *J Exp Biol*. 2007 Nov 1;210(21):3763–70.
- 437 7. Reynolds AM. Lévy flight patterns are predicted to be an emergent property of a bumblebees' foraging
438 strategy. *Behav Ecol Sociobiol*. 2009 Nov;64(1):19–23.
- 439 8. Ohashi K, Thomson JD, D'Souza D. Trapline foraging by bumble bees: IV. Optimization of route
440 geometry in the absence of competition. *Behav Ecol*. 2007 Jan;18(1):1–11.
- 441 9. Pyke GH, Cartar RV. The Flight Directionality of Bumblebees: Do They Remember Where They Came
442 from? *Oikos*. 1992;65(2):321–7.
- 443 10. Pyke GH. Optimal foraging in bumblebees and coevolution with their plants. *Oecologia*. 1978 Jan
444 1;36(3):281–93.
- 445 11. Lihoreau M, Chittka L, Raine NE. Monitoring Flower Visitation Networks and Interactions
446 between Pairs of Bumble Bees in a Large Outdoor Flight Cage. Ollerton J, editor. PLOS ONE. 2016 Mar
447 16;11(3):e0150844.
- 448 12. Vallaey V, Tyson RC, Lane WD, Deleersnijder E, Hanert E. A Lévy-flight diffusion model to predict
449 transgenic pollen dispersal. *J R Soc Interface*. 2017 Jan 31;14(126):20160889.
- 450 13. Collett M, Chittka L, Collett TS. Spatial Memory in Insect Navigation. *Curr Biol*. 2013 Sep
451 9;23(17):R789–800.
- 452 14. Woodgate JL, Makinson JC, Lim KS, Reynolds AM, Chittka L. Life-Long Radar Tracking of
453 Bumblebees. Pratt SC, editor. PLOS ONE. 2016 Aug 4;11(8):e0160333.
- 454 15. Brebner JS, Makinson JC, Bates OK, Rossi N, Lim KS, Dubois T, et al. Bumble bees strategically use
455 ground level linear features in navigation. *Anim Behav*. 2021 Sep 1;179:147–60.
- 456 16. Menzel R, Lehmann K, Manz G, Fuchs J, Koblösky M, Greggers U. Vector integration and novel
457 shortcutting in honeybee navigation. *Apidologie*. 2012 May 1;43(3):229–43.
- 458 17. Lihoreau M, Raine NE, Reynolds AM, Stelzer RJ, Lim KS, Smith AD, et al. Radar Tracking and
459 Motion-Sensitive Cameras on Flowers Reveal the Development of Pollinator Multi-Destination Routes
460 over Large Spatial Scales. Collett T, editor. PLoS Biol. 2012 Sep 20;10(9):e1001392.
- 461 18. Woodgate JL, Makinson JC, Lim KS, Reynolds AM, Chittka L. Continuous Radar Tracking Illustrates
462 the Development of Multi-destination Routes of Bumblebees. *Sci Rep*. 2017 Dec;7(1):17323.
- 463 19. Lihoreau M, Chittka L, Raine NE. Travel Optimization by Foraging Bumblebees through
464 Readjustments of Traplines after Discovery of New Feeding Locations. *Am Nat*. 2010 Dec;176(6):744–
465 57.
- 466 20. Lihoreau M, Chittka L, Le Comber SC, Raine NE. Bees do not use nearest-neighbour rules for
467 optimization of multi-location routes. *Biol Lett*. 2012 Feb 23;8(1):13–6.

- 468 21. Reynolds AM, Lihoreau M, Chittka L. A Simple Iterative Model Accurately Captures Complex
469 Trapline Formation by Bumblebees Across Spatial Scales and Flower Arrangements. Ayers J, editor.
470 PLoS Comput Biol. 2013 Mar 7;9(3):e1002938.
- 471 22. Dubois T, Pasquaretta C, Barron AB, Gautrais J, Lihoreau M. A model of resource partitioning
472 between foraging bees based on learning. PLOS Comput Biol. 2021 Jul 28;17(7):e1009260.
- 473 23. Von Frisch K. Die Tänze der Bienen. In: Von Frisch K, editor. Tanzsprache und Orientierung der
474 Bienen [Internet]. Berlin, Heidelberg: Springer; 1965 [cited 2022 Aug 30]. p. 3–330. Available from:
475 https://doi.org/10.1007/978-3-642-94916-6_2
- 476 24. Capaldi EA, Smith AD, Osborne JL, Fahrbach SE, Farris SM, Reynolds DR, et al. Ontogeny of
477 orientation flight in the honeybee revealed by harmonic radar. Nature. 2000 Feb;403(6769):537–40.
- 478 25. Edwards AM, Phillips RA, Watkins NW, Freeman MP, Murphy EJ, Afanasyev V, et al. Revisiting
479 Lévy flight search patterns of wandering albatrosses, bumblebees and deer. Nature. 2007
480 Oct;449(7165):1044–8.
- 481 26. Benhamou S. How Many Animals Really Do the Lévy Walk? Ecology. 2007;88(8):1962–9.
- 482 27. Ohashi K, Leslie A, Thomson JD. Trapline foraging by bumble bees: V. Effects of experience and
483 priority on competitive performance. Behav Ecol. 2008;19(5):936–48.
- 484 28. Lihoreau M, Chittka L, Raine NE. Trade-off between travel distance and prioritization of high-
485 reward sites in traplining bumblebees: Distance reward trade-off in bees. Funct Ecol. 2011
486 Dec;25(6):1284–92.
- 487 29. Stout JC. Does size matter? Bumblebee behaviour and the pollination of *Cytisus scoparius* L.
488 (Fabaceae). Apidologie. 2000 Jan;31(1):129–39.
- 489 30. Gautrais J, Jost C, Soria M, Campo A, Motsch S, Fournier R, et al. Analyzing fish movement as a
490 persistent turning walker. J Math Biol. 2009 Mar;58(3):429–45.
- 491 31. Szabados T. An elementary introduction to the Wiener process and stochastic integrals
492 [Internet]. arXiv; 2010 [cited 2022 Sep 2]. Available from: <http://arxiv.org/abs/1008.1510>
- 493 32. Degond P, Motsch S. Large Scale Dynamics of the Persistent Turning Walker Model of Fish
494 Behavior. J Stat Phys. 2008 Jun;131(6):989–1021.
- 495 33. Cattiaux P, Chafai D, Motsch S. Asymptotic analysis and diffusion limit of the Persistent Turning
496 Walker Model. Asymptot Anal. 2010 Mar;67(1–2):17–31.
- 497 34. Weber C, Radtke PK, Schimansky-Geier L, Hänggi P. Active motion assisted by correlated
498 stochastic torques. 2011 [cited 2022 Sep 9]; Available from: <https://arxiv.org/abs/1105.3363>
- 499 35. Daltorio KA, Tietz BR, Bender JA, Webster VA, Szczecinski NS, Branicky MS, et al. A model of
500 exploration and goal-searching in the cockroach, *Blaberus discoidalis*. Adapt Behav. 2013
501 Oct;21(5):404–20.
- 502 36. Nötel J, Sokolov IM, Schimansky-Geier L. Diffusion of active particles with stochastic torques
503 modeled as α -stable noise. J Phys Math Theor. 2017 Jan 20;50(3):034003.
- 504 37. Du G, Kumari S, Ye F, Podgornik R. Model of metameric locomotion in smooth active directional
505 filaments with curvature fluctuations. Europhys Lett. 2021 Dec;136(5):58003.

- 506 38. Heinze S, Narendra A, Cheung A. Principles of Insect Path Integration. *Curr Biol*. 2018 Sep
507 10;28(17):R1043–58.
- 508 39. Pasquaretta C, Dubois T, Gomez-Moracho T, Delepoulle VP, Le Loc’h G, Heeb P, et al. Analysis of
509 temporal patterns in animal movement networks. *Methods Ecol Evol*. 2021;12(1):101–13.
- 510 40. Osborne JL, Smith A, Clark SJ, Reynolds DR, Barron MC, Lim KS, et al. The Ontogeny of Bumblebee
511 Flight Trajectories: From Naïve Explorers to Experienced Foragers. Smaghe G, editor. *PLoS ONE*. 2013
512 Nov 12;8(11):e78681.
- 513 41. Mwaffo V, Keshavan J, L. Hedrick T, Humbert S. Detecting intermittent switching leadership in
514 coupled dynamical systems. *Sci Rep*. 2018 Jul 9;8(1):10338.
- 515 42. Mwaffo V, Anderson RP, Butail S, Porfiri M. A jump persistent turning walker to model zebrafish
516 locomotion. *J R Soc Interface*. 2015 Jan 6;12(102):20140884.
- 517 43. Mwaffo V, Butail S, Porfiri M. In-silico experiments of zebrafish behaviour: modeling swimming in
518 three dimensions. *Sci Rep*. 2017 Jan 10;7(1):39877.
- 519 44. Brown AA, Brown MF, Folk SR, Utter BA. Archerfish respond to a hunting robotic conspecific. *Biol*
520 *Cybern*. 2021 Dec 1;115(6):585–98.
- 521 45. Khan A, Al-Abri S, Mishra V, Zhang F. A bio-inspired localization-free stochastic coverage
522 algorithm with verified reachability. *Bioinspiration Ampmathsemicolon Biomim*. 2021
523 Jul;16(5):056009.
- 524 46. Kapustjansky A, Chittka L, Spaethe J. Bees use three-dimensional information to improve target
525 detection. *Naturwissenschaften*. 2010 Feb;97(2):229–33.
- 526 47. Klein S, Pasquaretta C, Barron AB, Devaud JM, Lihoreau M. Inter-individual variability in the
527 foraging behaviour of traplining bumblebees. *Sci Rep*. 2017 Jul 4;7(1):4561.
- 528 48. Chittka L, Dyer AG, Bock F, Dornhaus A. Bees trade off foraging speed for accuracy. *Nature*. 2003
529 Jul;424(6947):388–388.

530

531 **Supporting information**

532 **S1 Fig. Variability of each observable across individuals in the experimental dataset. (A)** Loop lengths (m)
533 for each bee, as defined in Fig. 3 in the main text. Boxplots, show the median (middle line), 25 and 75%
534 quantiles (box), range of data within 1.5 interquartile deviations (whiskers), and outliers (dots). **(B)** Same
535 as A but for the loop extension (maximum distance between the nest and the individual). **(C)** Same as A,
536 but for the number of re-departures per 100m traveled. A re-departure is defined as three consecutive
537 positions such that the second position is closer to the nest than the first one, but the third is again further

538 away than the second. **(D)** Same as A but for the intersections (number of times the loop intersects with
539 itself)

540 **S2 Text. Raw results and figures**

541 **S3 Data and code sources for analysis and simulations.**